

Nanosecond pulse and dual-wavelength Q-switched 1.5 μm fiber laser using MAX phase $\text{Cr}_2\text{TiAlC}_2$ saturable absorber

Ahmed Shakir AL-HITI^{1*} and Hiba HASSAN²

1. Department of Electrical Engineering, Faculty of Engineering, University of Anbar, Anbar 31001, Iraq

2. Department of Laser and Optoelectronics Engineering, University of Technology-Iraq, Baghdad, Iraq

(Received 12 December 2023; Revised 21 July 2024)

©Tianjin University of Technology 2025

We demonstrated a new type of MAX phase material, chromium titanium aluminum carbide ($\text{Cr}_2\text{TiAlC}_2$) polymer film, to generate a passively Q-switched erbium-doped fiber laser (EDFL). The film thickness was measured to be around 45 μm , which was fabricated using the embedding method with polyvinyl alcohol (PVA) polymer as hoster. The saturable absorber (SA) film demonstrates a dual-wavelength passively Q-switched EDFL which operates at 1 531 nm and 1 560.19 nm, respectively. The Q-switching pulse duration could be varied from 2.46 μs to 770 ns, while the repetition rate varied from 92.76 kHz to 106.6 kHz with an increasing input pumping range from 154 mW to 300 mW. The maximum output power and pulse energy of 15.05 mW and 141.18 nJ were obtained at the maximum input power of 300 mW, respectively.

Document code: A **Article ID:** 1673-1905(2025)01-0007-6

DOI <https://doi.org/10.1007/s11801-025-3283-x>

1. Introduction

Q-switched fiber lasers are highly sought after laser sources for a wide range of systems like medical systems, micromachining, and sensors, due to their ability to generate high-energy pulses^[1]. Recently, a Q-switched laser operating in the 1.5 μm wavelength region has received interest because of its different systems like medical applications and optical communications, etc. Passive and active switching techniques are typically used in pulsed fiber laser applications. Although active Q-switching or mode-locking of a fiber laser can provide stable pulsed operation, this generally requires expensive optical components and a complex electronic device^[2]. One basic way to achieve passive Q-switched operation is to use an optical component known as a saturable absorber (SA) that is inserted into the laser cavity to generate pulses in different infrared spectral regions.

Fiber lasers have used several materials as passive devices to generate pulses that operate in regions of different wavelengths. These materials include semiconductor saturable absorber mirrors (SESAMs)^[3], graphene^[4], carbon nanotubes (CNTs)^[5], black phosphorus (BP)^[6], topological insulators (TIs)^[7], Sb_2Te_3 , Bi_2Se_3 , Bi_2Te_3 , etc, and transition metal dichalcogenides (TMDs)^[8], WS_2 , WSe_2 , MoSe_2 , MoS_2 , etc. However, SESAMs have a narrow wavelength range, so they are of limited use^[9]. Graphene has a low SA around 2.3% at 1 550 nm^[10]. CNTs suffer low absorption because of their tube size^[11].

While BP is a hydrophilic material and its interaction with humid environments will affect its performance^[12]. The TIs materials have a difficult preparation process due to the existence of two various elements, while TMDs have complex fabrication and low damage threshold^[13]. Besides, the development of fiber-optical technologies also led to the notion of so-called artificial SAs. So, artificial SA is based mainly on fiber-optical material and its optical nonlinear effects. This type of SA can be produced from many methods, such as polarization effects, spatial effects, spectral effects, and reflector effects like nonlinear optical loop mirror (NOLM) and nonlinear amplifying loop mirror (NALM)^[14].

Recently, the MAX phase seed material for the fabrication of MXene has also aroused the interest of many authors around the world. MAX phase can be formulated utilizing $\text{M}_{n+1}\text{AX}_n$, as M is a transition metal (like Nb, V, Ti, etc), and A represents an element from group A (like Sn, Al, etc). X is referred to as nitrogen and carbon and n is equal to 1, 2, or 3^[15]. These materials have a special atomic arrangement with ceramic and metal because of their structure. It also has high resistance to temperature and oxidation with excellent thermal conductivity, as these properties make it useful in various applications, such as high-temperature devices and nuclear engineering^[16]. The chromium titanium aluminum carbide ($\text{Cr}_2\text{TiAlC}_2$) contains Cr and Ti atoms in the M_3AX_2 crystal structure^[17]. It showed also improved high-temperature mechanical characteristics with good oxidation resistance^[18]. The

* Ahmed Shakir AL-HITI is a lecturer in University of Anbar. He received his Ph.D. degree from University of Malaya in 2021. His research interests are mainly in optical communications, lasers, laser-plasma accelerators, and materials science. E-mail: ahmed.s.abd@uoanbar.edu.iq.

$\text{Cr}_2\text{TiAlC}_2$ has an excellent ability to Na_2SO_4 melts^[19]. $\text{Cr}_2\text{TiAlC}_2$ has been used in many applications due to its excellent properties, including photonics, plasmonics, and energy storage. Moreover, it is highly stable in all ambient conditions compared to other two-dimensional materials, and can be fabricated in simple and inexpensive methods. Therefore, it has demonstrated attractive functionalities like solution processability, optical properties, high electronic conductivity, etc. $\text{Cr}_2\text{TiAlC}_2$ also has a unique crystalline structure among other MAX phase members that makes it stable at high temperatures and good hot corrosion resistance.

In this paper, we demonstrated a passively Q-switched erbium-doped fiber laser (EDFL) operating at 1.5 μm regions utilizing $\text{Cr}_2\text{TiAlC}_2$ -based SA. The SA film was fabricated using an embedding method into polyvinyl alcohol (PVA) to form a thin film. The SA film was produced dual-wavelength operating at 1 560.71 nm and 1 562.27 nm, respectively.

2. Fabrication and characterization of $\text{Cr}_2\text{TiAlC}_2$ thin film

Many fabricating processes suffer from drawbacks affecting laser performance, including mechanical exfoliation, electrochemical exfoliation, etc. So, we utilized the embedding method to create the SA film with controllable concentration and insensitive to polarization. In this paper, we utilized PVA as a host because of its remarkable physical properties to produce an absorber film. The 1 g of PVA was poured into 100 mL of deionized (DI) water and stirred at 400 rpm for 2 h at room temperature. Afterward, 10 mL of the prepared PVA solution was moved into a glass beaker. The 10 mg of the proposed material was cast in 10 mL of pre-made PVA. Then, it was agitated for 250 min at 45 °C. After 250 min, prepared $\text{Cr}_2\text{TiAlC}_2$ PVA was dropped in a glass dish for 96 h to produce a thin layer of $\text{Cr}_2\text{TiAlC}_2$ PVA. The SA film is cut into small pieces (1 mm×1 mm) to be used as SA. The fabricated $\text{Cr}_2\text{TiAlC}_2$ -based SA was attached to a clean FC/PC fiber ferrule with an index-matching gel.

The X-ray diffraction (XRD) analysis of the $\text{Cr}_2\text{TiAlC}_2$ thin film is shown in Fig.1(a). The XRD pattern was measured in the range from 10° to 70° and indicates different peaks. The first peak is located at 19.5° which indicates the creation of the crystalline structure of PVA in the SA film. Other peaks were witnessed at various positions of 10.11°, 20.09°, 29.99°, 36.16°, 39.31°, 41.20°, 43.01°, 44.64°, 50.81°, 55.22°, 59.56°, and 64.30°, which correspond to (002), (004), (005), (006), (007), (009), (0010), (017), (018), (019), and (110) planes obtained because of the characteristics of TiC and Cr_2AlC incremented with the incrementing temperature with PVA polymer. The SA film has been analyzed using a scanning electron microscope (SEM), as shown in Fig.1(b). The $\text{Cr}_2\text{TiAlC}_2$ nanoparticles were distributed uniformly with the PVA polymer. Some particles are also shown in the SEM image that belong to the $\text{Cr}_2\text{TiAlC}_2$

material.

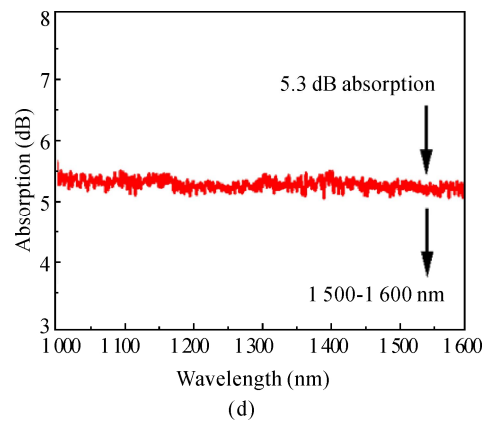
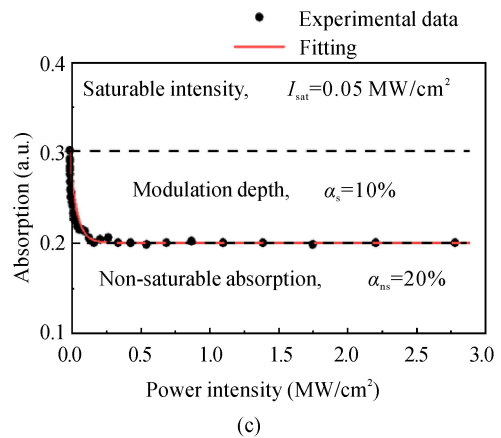
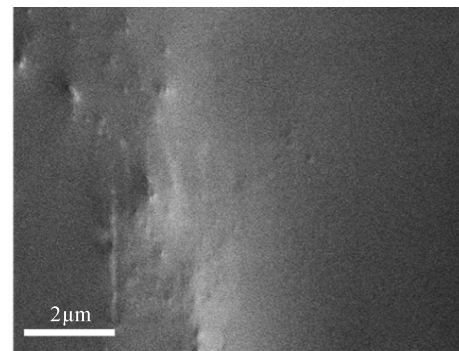
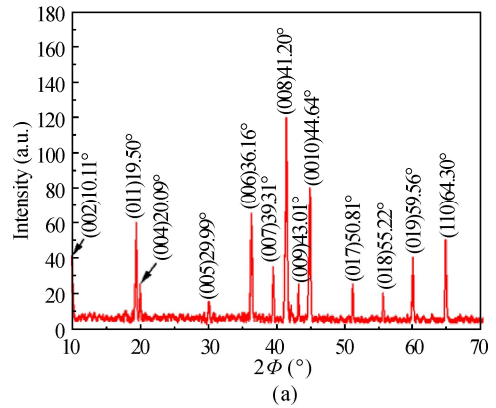


Fig.1 Characterization of SA film: (a) XRD analysis; (b) SEM image; (c) Nonlinear absorption; (d) Linear absorption

Fig.1(c) shows the nonlinear optical absorption of $\text{Cr}_2\text{TiAlC}_2$ PVA SA. It is obtained utilizing a balanced twin detector technique. This method was produced based on an optical coupler (OC), optical attenuator (OA), erbium-doped fiber amplifier (EDFA), and ultrashort pulse source. An ultrashort pulse was used as the input source operating at 1562 nm with a picosecond pulse width. The OA and EDFA were used to change laser intensity. A 3 dB coupler has been utilized to split the laser and analyze the performance. The saturation intensity (I_{sat}), non-saturable absorption (α_{ns}), and saturable absorption (α_0) of the proposed SA film were estimated to be 10%, 0.05 mW/cm², and 20%, respectively. The linear absorption profile of the proposed SA film achieved an optical absorption of about 5.3 dB from 1500 nm to 1600 nm wavelength (see Fig.1(d)).

3. Laser configuration

The laser setup of the Q-switched EDFL ring cavity is depicted in Fig.2. An erbium-doped fiber (EDF) with a total length of 2 m was used as the active gain medium. The EDF has a 4 μm core diameter and 23 dB/m ion absorption loss. A 980 nm laser diode (LD) was used to pump into the laser cavity utilizing a 980/1550 nm wavelength division multiplexer (WDM). An isolator (ISO) was used to maintain the unidirectional laser distribution within the cavity, while a 50:50 OC was utilized for extracting out 50% to evaluate the laser performance. This coupler was utilized to provide optimal output power for the proposed SA thin film. The $\text{Cr}_2\text{TiAlC}_2$ -PVA film was sandwiched between two fiber connectors to act as SA. A polarization controller (PC) was used to improve the polarization state because $\text{Cr}_2\text{TiAlC}_2$ SA material is highly polarization sensitive due to its high optical anisotropic property that plays a crucial role in light manipulation owing to birefringence phenomena. The total cavity length was 8.7 m. Time traces, power output, and optical spectrum of the proposed laser were obtained by a 350 MHz oscilloscope (OSC), optical power meter (OPM), 7.8 GHz radio frequency spectrum analyzer (RFSA), and optical spectrum analyzer (OSA) with a model of Thorlabs PM100D, Anritsu MS2683A, and Anritsu MS9710C, respectively.

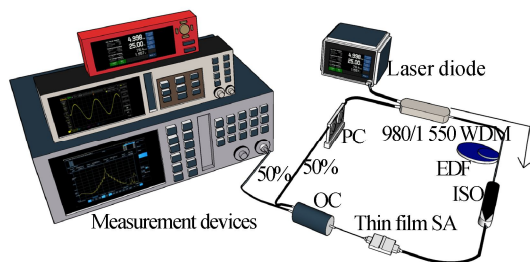


Fig.2 Laser experiment with $\text{Cr}_2\text{TiAlC}_2$ -PVA thin film

4. Results and discussion

The EDFL cavity was tested and investigated without SA

to obtain the threshold input power. The continuous wave (CW) operation of our cavity was achieved at a threshold input power of 10 mW. By inserting the $\text{Cr}_2\text{TiAlC}_2$ PVA SA and increasing the input power to 154 mW, with the PC precisely adjusted, the CW output laser was converted to a Q-switched operation with a stable pulse train. Fig.3(a) shows the pulse train of a Q-switched EDFL operation at a maximum input power of 300 mW. The pulse train shows uniform and high stability pulses. It has a 770 ns pulse width with a 106.6 kHz pulse rate which corresponds to a time interval of 9.38 μs . The optical damage threshold has been analyzed and is estimated to be higher than 300 mW. The experimental result of the pulse train by OSC was obtained at the maximum pumping input power, as shown in Fig.3(b). The single pulse envelope of $\text{Cr}_2\text{TiAlC}_2$ PVA SA is shown in Fig.3(c). It has a pulse width of 770 ns with a repetition rate of 106.6 kHz, respectively.

The output spectra of the proposed laser were obtained via OSA at a resolution of 0.07 nm, as given in Fig.4. When a 300 mW laser was pumped, a dual-wavelength was obtained. This is because sufficient laser power was supplied into the cavity with a good level of SA saturation. The dual-wavelength Q-switched EDFL (blue color) was realized at 1531 nm and 1560.19 nm wavelengths with a 3 dB bandwidth of 1.2 nm and 1 nm, respectively. The laser wavelength separation between two peaks is 29.19 nm with a laser wavelength range from 1515 nm to 1580 nm, respectively.

To analyze the stability of Q-switched EDFL operation, the radio frequency (RF) spectrum was gauged at a resolution of 1 kHz (see Fig.5(a)). At a 106.6 kHz frequency, a single strong peak corresponding to a time interval of 9.38 μs was observed in the RFSA monitor tracing with a span of 1.93 MHz. This means that the laser output was in a stable Q-switching state. Besides, the signal-to-noise ratio (SNR) was gauged at 72 dB. The RF spectra versus laser pumping are shown in Fig.5(b). The Q-switched laser shows a good pulse with small standard deviations and excellent stability at around 72 dB.

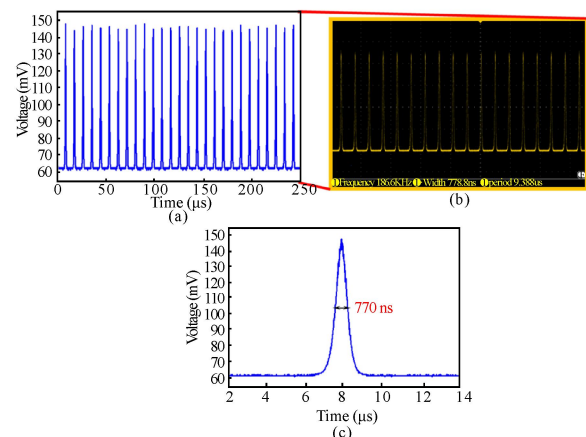


Fig.3 Pulse train of the Q-switched EDF laser: (a) Calculation of the pulse train; (b) Snapshot of the oscilloscope device; (c) Single pulse envelope of the proposed Q-switched pulses

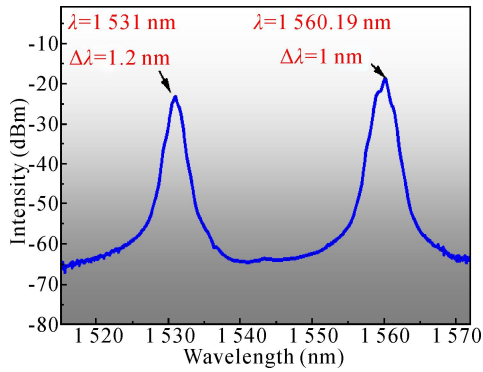


Fig.4 Output spectrum of the Q-switched EDF laser

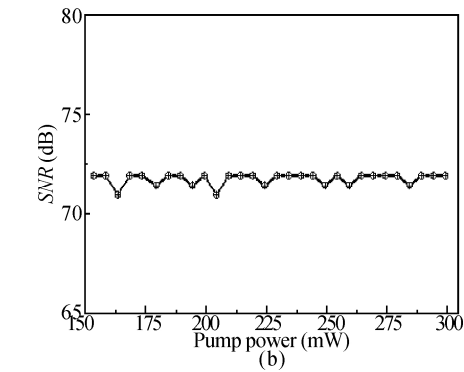
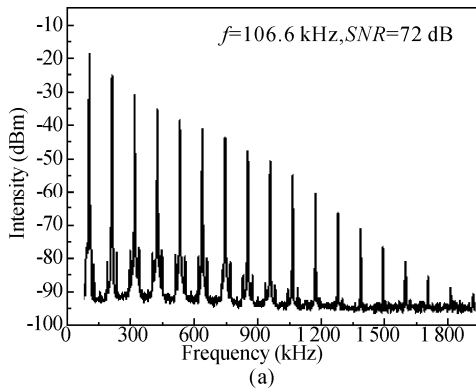


Fig.5 RF spectrum of the proposed laser: (a) RF spectrum; (b) SNR gauged versus laser pumping

We subsequently gauged the repetition rate and pulse duration of Q-switched laser operation based on different input power as given in Fig.6(a). The repetition rate raised from 92.76 kHz to 106.6 kHz while the pulse duration decreased from 2.46 μ s to 0.77 μ s, as input power was increased from 154 mW to 300 mW. Moreover, the pulse energy and output power of the laser were measured as a function of input power, as exhibited in Fig.6(b). The pulse energy of the laser raised from 57.99 nJ to 141.18 nJ, while the output power also increased from 5.38 mW to 15.05 mW, respectively. The peak power of the proposed Q-switched laser is shown in Fig.6(c). The peak power of the proposed laser has been achieved from 23.57 mW to 183.35 mW at the same pump power range, respectively.

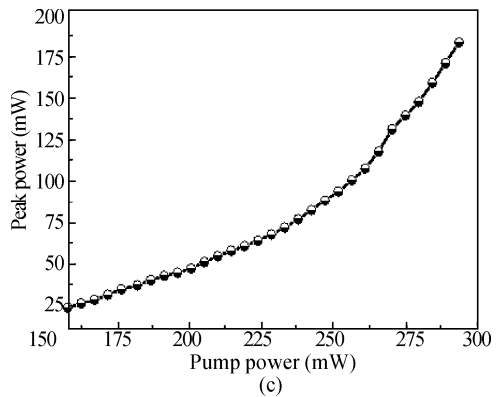
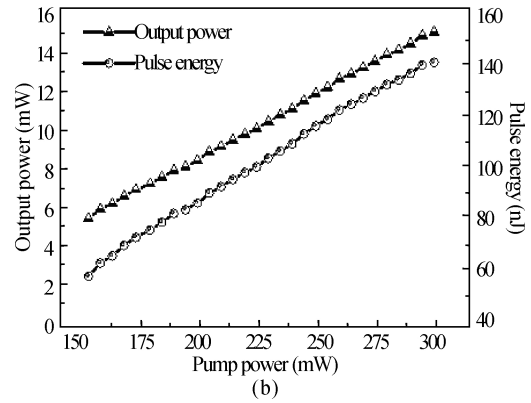
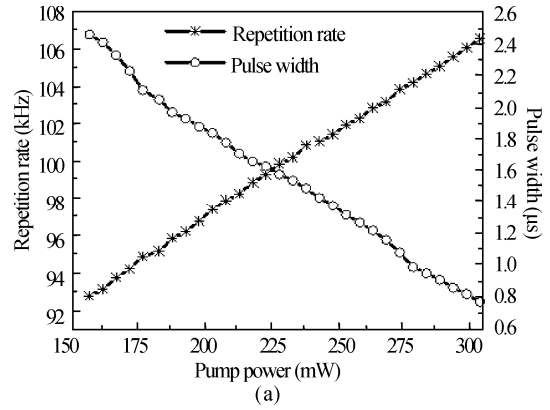


Fig.6 The proposed laser performance: (a) Repetition rate and pulse width versus laser pumping; (b) Output power and pulse energy versus laser pumping; (c) Peak power versus laser pumping

Finally, we analyzed the long-term stability of Q-switched pulses by gauging the laser spectrum for 1 h in the laboratory, as exhibited in Fig.7. The dual-wavelength Q-switched laser was observed to be constant at 1531 nm and 1560.19 nm with a peak power of -23.71 dB and -18.82 dB, respectively. The spectrum was monitored, and no change occurred which indicates the Q-switched EDFL operation was stable for 60 min in the laboratory. This experiment was repeated after two weeks, the results remained the same indicating that no degradation or change in the material phase because Cr₂TiAlC₂ material is stable at ambient conditions unlike SESAM. Besides, it was embedded in polymer (PVA)

thin film that makes the SA has long term stability without changing its structure or properties. All previously reported dual-wavelength Q-switched lasers were compared with our proposed laser, as shown in Tab.1. The proposed laser operates at 1 530 nm and 1 560 nm, respectively, as our work has a longer wavelength spacing of 29.19 nm compared to previous works, which makes it

suitable for various applications. Also, the proposed laser achieved a pulse duration of about 770 ns with an SNR of 72 dB, which is much better than previously reported works due to the high SA efficiency of the proposed material. The proposed laser achieved high efficiency in terms of repetition rate and pulse energy. This indicates that our laser has high performance operating at 1.55 μm region.

Tab.1 Performance comparison of all-fiber dual-wavelength Q-switched laser to previous works at 1.55 μm

SA material	Integration platform	Dual wavelength	Maximum repetition rate	Pulse duration	Maximum pulse energy	SNR	Ref.
GO	D-shaped fiber	1 549.6—1 558.6 nm	65.27 kHz	2.9 μs	15.17 nJ	-	[20]
CaCO ₃	Thin film	1 563.5—1 564.9 nm	21.3 kHz	18.74 μs	2.82 nJ	25 dB	[21]
MoSSe	Thin film	1 532.2—1 532.8 nm	90 kHz	1.78 μs	257 nJ	50 dB	[22]
SWNT	Thin film	1 532—1 558 nm	66.2 kHz	3.3 μs	0.5 nJ	-	[23]
MWCNTs	Thin film	1 532.32—1 556.97 nm	78 kHz	5.24 μs	11.97 nJ	26 dB	[24]
SESAM	Thin film	1 556.83—1 562.11 nm	58.57 kHz	17.07 μs	-	49 dB	[25]
Cr ₂ TiAlC ₂	Thin film	1 531—1 560.19 nm	106.6 kHz	0.77 μs	141.18 nJ	72 dB	This work

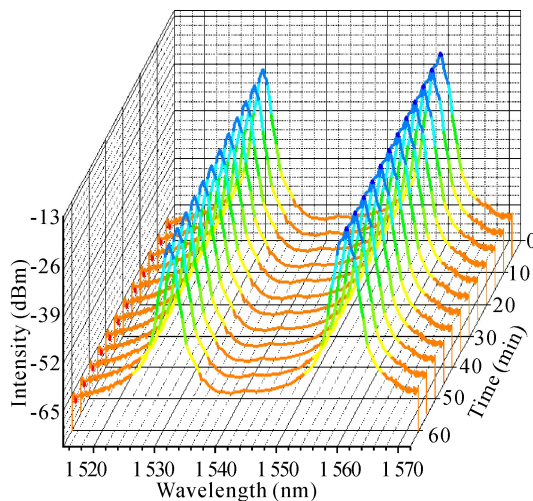


Fig.7 Long-term evaluation of laser wavelength for 1 h

5. Conclusion

A passive dual-wavelength Q-switched EDFL was experimentally demonstrated and investigated, utilizing Cr₂TiAlC₂-PVA as SA. The fabrication of Cr₂TiAlC₂-based SA was done by embedding Cr₂TiAlC₂ powder into a PVA solution to form an absorber film. The nonlinear absorption of the proposed Cr₂TiAlC₂-PVA film achieved a 10% saturable absorption with a 0.05 MW/cm² saturation intensity. The Q-switched EDFL operation showed that the minimum pulse duration and highest pulse rate are 770 ns and 106.6 kHz at a maximum input power of 300 mW, respectively. The proposed laser can be applied in photonics applications.

Ethics declarations

Conflicts of interest

The authors declare no conflict of interest.

References

- [1] LI S, YIN Y, OUYANG Q, et al. Nanosecond passively Q-switched fibre laser using a NiS₂ based saturable absorber[J]. Optics express, 2019, 27(14): 19843-19851.
- [2] PEDRUZZI E, SILVA L C B, LEAL-JUNIOR A G, et al. Generation of a multi-wavelength Brillouin erbium fiber laser with low threshold in multiple frequency spacing configurations[J]. Optical fiber technology, 2022, 69: 102832.
- [3] LV Z, YANG Z, LI F, et al. SESAM mode-locked all-polarization-maintaining fiber linear cavity ytterbium laser source with spectral filter as pulse shaper[J]. Laser physics, 2018, 28(12): 125103.
- [4] SOBON G, SOTOR J, ABRAMSKI K M. All-polarization maintaining femtosecond Er-doped fiber laser mode-locked by graphene saturable absorber[J]. Laser physics letters, 2012, 9(8): 581.
- [5] LI X, WU K, SUN Z, et al. Single-wall carbon nanotubes and graphene oxide-based saturable absorbers for low phase noise mode-locked fiber lasers[J]. Scientific reports, 2016, 6: 25266.
- [6] LI J, LUO H, ZHAI B, et al. Black phosphorus: a two-dimension saturable absorption material for mid-infrared Q-switched and mode-locked fiber lasers[J]. Scientific reports, 2016, 6: 30361.
- [7] JHON Y I, LEE J, JHON Y M, et al. Topological insulators for mode-locking of 2- μm fiber lasers[J]. IEEE journal of selected topics in quantum electronics, 2018, 24(5): 1-8.
- [8] LI L, PANG L, WANG R, et al. Ternary transition metal dichalcogenides for high power vector dissipative soliton ultrafast fiber laser[J]. Laser & photonics reviews, 2022, 16(2): 2100255.
- [9] AL-HITI A S, APSARI R, YASIN M, et al. Nanosecond Q-switched pulse generation using poly (3,4-ethylenedioxythiophene): poly (4-styrenesulfonate)

- thin film as saturable absorber[J]. *Infrared physics & technology.*, 2021, 116: 103788.
- [10] AL-HITI A S, YASIN M, NAJM M M, et al. Femtosecond mode-locked 1.5 μm fiber laser based on PEDOT: PSS as saturable absorber[J]. *Optics communications*, 2023: 129926.
- [11] AL-HITI A S, YASIN M, HARUN S W. MAX phase V_4AlC_3 for generating Q-switched pulses in 2 μm region[J]. *Optik*, 2023, 288: 171148.
- [12] AL-HITI A S, YASIN M, HARUN S W. Nanosecond Q-switched laser with PEDOT: PSS saturable absorber[J]. *Applied optics*, 2022, 61(6): 1292-1299.
- [13] AL-HITI A S, YASIN M, HARUN S W. Poly(3, 4-ethylenedioxythiophene): poly(styrenesulfonate) spin-coated onto polyvinyl alcohol film as saturable absorber for generating Q-switched laser at 1.5 μm region[J]. *Optical fiber technology*, 2022, 68: 102763.
- [14] KOBTSEV S M. Artificial saturable absorbers for ultrafast fibre lasers[J]. *Optical fiber technology*, 2022, 68: 102764.
- [15] BARSOUM M W. The MN^+1AXN phases: a new class of solids: thermodynamically stable nanolaminates[J]. *Progress in solid state chemistry*, 2000, 28(1-4): 201-281.
- [16] HOFFMAN E N, VINSON D W, SINDELAR R L, et al. MAX phase carbides and nitrides: properties for future nuclear power plant in-core applications and neutron transmutation analysis[J]. *Nuclear engineering and design*, 2012, 244: 17-24.
- [17] LIU Z, WU E, WANG J, et al. Crystal structure and formation mechanism of $(\text{Cr}_{2/3}\text{Ti}_{1/3})_3\text{AlC}_2$ MAX phase[J]. *Acta materialia*, 2014, 73: 186-193.
- [18] LIU Z, YANG J, QIAN Y, et al. High temperature oxidation behavior of quaternary ordered $(\text{Cr}_{2/3}\text{Ti}_{1/3})_3\text{AlC}_2$ -based MAX ceramic[J]. *Corrosion science*, 2021, 183: 109317.
- [19] LI X, WANG S, WU G, et al. Oxidation and hot corrosion behaviors of MAX-phase Ti_3SiC_2 , Ti_2AlC , Cr_2AlC [J]. *Ceramics international*, 2022, 48(18): 26618-26628.
- [20] NOOR S, AHMAD B A, ROSOL A H A, et al. Dual-wavelength Q-switched erbium-doped fiber laser using an SMF-MMF-SMF structure and graphene oxide[J]. *Optoelectronics letters*, 2022, 18(11): 668-672.
- [21] JASEM I N, ABDULLAH H H, JALAL A M. Dual-wavelength passively Q-switched erbium-doped fiber laser incorporating calcium carbonate nanoparticles as saturable absorber[J]. *Journal of nanotechnology*, 2023.
- [22] LI G, HE J, YAN B, et al. Dual-wavelength passively Q-switched Er-doped fiber laser based on a MoS₂ saturable absorber[J]. *OSA continuum*, 2019, 2(1): 192-200.
- [23] LIU L, ZHENG Z, ZHAO X, et al. Dual-wavelength passively Q-switched erbium doped fiber laser based on an SWNT saturable absorber[J]. *Optics communications*, 2013, 294: 267-270.
- [24] ZUIKAFLY S N F, AHMAD F, IBRAHIM M H, et al. Dual-wavelength passively Q-switched erbium-doped fiber laser with MWCNTs slurry as saturable absorber[J]. *Photonics letters of Poland*, 2016, 8(4): 98-100.
- [25] CHEN S, LU B, WEN Z, et al. Single/dual-wavelength switchable and tunable passively Q-switched erbium-doped fiber laser[J]. *Infrared physics & technology*, 2020, 111: 103519.